

Study of Exclusive Radiative B Meson Decays

T. E. Coan,¹ V. Fadeyev,¹ Y. Maravin,¹ I. Narsky,¹ R. Stroynowski,¹ J. Ye,¹ T. Wlodek,¹ M. Artuso,² R. Ayad,² C. Boulahouache,² K. Bukin,² E. Dambasuren,² S. Karamnov,² S. Kopp,² G. Majumder,² G. C. Moneti,² R. Mountain,² S. Schuh,² T. Skwarnicki,² S. Stone,² G. Viehhauser,² J.C. Wang,² A. Wolf,² J. Wu,² S. E. Csorna,³ I. Danko,³ K. W. McLean,³ Sz. Márka,³ Z. Xu,³ R. Godang,⁴ K. Kinoshita,^{4,*} I. C. Lai,⁴ S. Schrenk,⁴ G. Bonvicini,⁵ D. Cinabro,⁵ L. P. Perera,⁵ G. J. Zhou,⁵ G. Eigen,⁶ E. Lipeles,⁶ M. Schmidtler,⁶ A. Shapiro,⁶ W. M. Sun,⁶ A. J. Weinstein,⁶ F. Würthwein,^{6,†} D. E. Jaffe,⁷ G. Masek,⁷ H. P. Paar,⁷ E. M. Potter,⁷ S. Prell,⁷ V. Sharma,⁷ D. M. Asner,⁸ A. Eppich,⁸ T. S. Hill,⁸ D. J. Lange,⁸ R. J. Morrison,⁸ R. A. Briere,⁹ B. H. Behrens,¹⁰ W. T. Ford,¹⁰ A. Gritsan,¹⁰ J. Roy,¹⁰ J. G. Smith,¹⁰ J. P. Alexander,¹¹ R. Baker,¹¹ C. Bebek,¹¹ B. E. Berger,¹¹ K. Berkelman,¹¹ F. Blanc,¹¹ V. Boisvert,¹¹ D. G. Cassel,¹¹ M. Dickson,¹¹ P. S. Drell,¹¹ K. M. Ecklund,¹¹ R. Ehrlich,¹¹ A. D. Foland,¹¹ P. Gaidarev,¹¹ L. Gibbons,¹¹ B. Gittelman,¹¹ S. W. Gray,¹¹ D. L. Hartill,¹¹ B. K. Heltsley,¹¹ P. I. Hopman,¹¹ C. D. Jones,¹¹ D. L. Kreinick,¹¹ M. Lohner,¹¹ A. Magerkurth,¹¹ T. O. Meyer,¹¹ N. B. Mistry,¹¹ E. Nordberg,¹¹ J. R. Patterson,¹¹ D. Peterson,¹¹ D. Riley,¹¹ J. G. Thayer,¹¹ P. G. Thies,¹¹ B. Valant-Spaight,¹¹ A. Warburton,¹¹ P. Avery,¹² C. Prescott,¹² A. I. Rubiera,¹² J. Yelton,¹² J. Zheng,¹² G. Brandenburg,¹³ A. Ershov,¹³ Y. S. Gao,¹³ D. Y.-J. Kim,¹³ R. Wilson,¹³ T. E. Browder,¹⁴ Y. Li,¹⁴ J. L. Rodriguez,¹⁴ H. Yamamoto,¹⁴ T. Bergfeld,¹⁵ B. I. Eisenstein,¹⁵ J. Ernst,¹⁵ G. E. Gladding,¹⁵ G. D. Gollin,¹⁵ R. M. Hans,¹⁵ E. Johnson,¹⁵ I. Karliner,¹⁵ M. A. Marsh,¹⁵ M. Palmer,¹⁵ C. Plager,¹⁵ C. Sedlack,¹⁵ M. Selen,¹⁵ J. J. Thaler,¹⁵ J. Williams,¹⁵ K. W. Edwards,¹⁶ R. Janicek,¹⁷ P. M. Patel,¹⁷ A. J. Sadoff,¹⁸ R. Ammar,¹⁹ A. Bean,¹⁹ D. Besson,¹⁹ R. Davis,¹⁹ N. Kwak,¹⁹ X. Zhao,¹⁹ S. Anderson,²⁰ V. V. Frolov,²⁰ Y. Kubota,²⁰ S. J. Lee,²⁰ R. Mahapatra,²⁰ J. J. O'Neill,²⁰ R. Poling,²⁰ T. Riehle,²⁰ A. Smith,²⁰ J. Urheim,²⁰ S. Ahmed,²¹ M. S. Alam,²¹ S. B. Athar,²¹ L. Jian,²¹ L. Ling,²¹ A. H. Mahmood,^{21,‡} M. Saleem,²¹ S. Timm,²¹ F. Wappler,²¹ A. Anastassov,²² J. E. Duboscq,²² K. K. Gan,²² C. Gwon,²² T. Hart,²² K. Honscheid,²² D. Hufnagel,²² H. Kagan,²² R. Kass,²² T. K. Pedlar,²² H. Schwarthoff,²² J. B. Thayer,²² E. von Toerne,²² M. M. Zoeller,²² S. J. Richichi,²³ H. Severini,²³ P. Skubic,²³ A. Undrus,²³ S. Chen,²⁴ J. Fast,²⁴ J. W. Hinson,²⁴ J. Lee,²⁴ N. Menon,²⁴ D. H. Miller,²⁴ E. I. Shibata,²⁴ I. P. J. Shipsey,²⁴ V. Pavlunin,²⁴ D. Cronin-Hennessy,²⁵ Y. Kwon,^{25,§} A.L. Lyon,²⁵ E. H. Thorndike,²⁵ C. P. Jessop,²⁶ H. Marsiske,²⁶ M. L. Perl,²⁶ V. Savinov,²⁶ D. Ugolini,²⁶ and X. Zhou²⁶

(CLEO Collaboration)

¹*Southern Methodist University, Dallas, Texas 75275*

²*Syracuse University, Syracuse, New York 13244*

³*Vanderbilt University, Nashville, Tennessee 37235*

⁴*Virginia Polytechnic Institute and State University, Blacksburg, Virginia 24061*

⁵*Wayne State University, Detroit, Michigan 48202*

⁶*California Institute of Technology, Pasadena, California 91125*

⁷*University of California, San Diego, La Jolla, California 92093*

⁸*University of California, Santa Barbara, California 93106*

⁹*Carnegie Mellon University, Pittsburgh, Pennsylvania 15213*

¹⁰*University of Colorado, Boulder, Colorado 80309-0390*

¹¹*Cornell University, Ithaca, New York 14853*

¹²*University of Florida, Gainesville, Florida 32611*

¹³*Harvard University, Cambridge, Massachusetts 02138*

¹⁴*University of Hawaii at Manoa, Honolulu, Hawaii 96822*

¹⁵*University of Illinois, Urbana-Champaign, Illinois 61801*

¹⁶*Carleton University, Ottawa, Ontario, Canada K1S 5B6*

and the Institute of Particle Physics, Canada

¹⁷*McGill University, Montréal, Québec, Canada H3A 2T8*

and the Institute of Particle Physics, Canada

¹⁸*Ithaca College, Ithaca, New York 14850*

¹⁹*University of Kansas, Lawrence, Kansas 66045*

²⁰*University of Minnesota, Minneapolis, Minnesota 55455*

²¹*State University of New York at Albany, Albany, New York 12222*

²²*Ohio State University, Columbus, Ohio 43210*

²³*University of Oklahoma, Norman, Oklahoma 73019*

²⁴*Purdue University, West Lafayette, Indiana 47907*

²⁵*University of Rochester, Rochester, New York 14627*

²⁶*Stanford Linear Accelerator Center, Stanford University, Stanford, California 94309*

(December 15, 1999)

We have investigated exclusive, radiative B meson decays to light mesons (ρ , ω , ϕ , $K^*(892)$, $K_2^*(1430)$) in 9.7×10^6 $B\bar{B}$ decays accumulated with the CLEO detector. The $B \rightarrow K^*(892)\gamma$ branching fractions are determined to be $\mathcal{B}(B^0 \rightarrow K^{*0}(892)\gamma) = (4.55_{-0.68}^{+0.72} \pm 0.34) \times 10^{-5}$ and $\mathcal{B}(B^+ \rightarrow K^{*+}(892)\gamma) = (3.76_{-0.83}^{+0.89} \pm 0.28) \times 10^{-5}$. We have searched for CP asymmetry in $B \rightarrow K^*(892)\gamma$ decays and measure $\mathcal{A}_{CP} = +0.08 \pm 0.13 \pm 0.03$. We also report the first observation of the decay $B \rightarrow K_2^*(1430)\gamma$ with a branching fraction of $(1.66_{-0.53}^{+0.59} \pm 0.13) \times 10^{-5}$ and determine $\mathcal{B}(B \rightarrow K_2^*(1430)\gamma)/\mathcal{B}(B \rightarrow K^*(892)\gamma) = 0.39_{-0.13}^{+0.15}$ consistent with only one of two available theoretical models. No significant evidence for the decays $B \rightarrow \rho\gamma$ and $B^0 \rightarrow \omega\gamma$ is found and we limit $\mathcal{B}(B \rightarrow (\rho/\omega)\gamma)/\mathcal{B}(B \rightarrow K^*(892)\gamma) < 0.32$ at 90% CL. We also find no evidence for the exotic decay $B^0 \rightarrow \phi\gamma$.

The radiative decays, $B \rightarrow K^*(892)\gamma$ and $B \rightarrow \rho\gamma$, occur via the quark transition $b \rightarrow s, d$ that involves a loop (“penguin”) diagram. In the Standard Model (SM), the loop amplitude is dominated by a virtual intermediate top quark coupling to a W boson and can be used to study the relative strength of the td and ts quark couplings (V_{td}/V_{ts}). The precise determination of the branching fraction of $B \rightarrow K^*\gamma$ [1] can be used to reduce the theoretical uncertainty in the extraction of V_{ub} from the measurement of the decay $B \rightarrow \rho\ell\nu$ [2,3]. The magnitudes of the couplings $|V_{ub}|$ and $|V_{td}/V_{ts}|$ are the lengths of two of the sides of the “unitarity triangle” used to test the SM mechanism of CP violation [4]. In addition the loop amplitude is sensitive to non-Standard Model (NSM) particles such as a supersymmetric charged Higgs; the interference of the SM and NSM amplitudes may result in observable direct CP -violating effects manifest in the charge asymmetry of $B \rightarrow K^*\gamma$ [5].

The observation of $B \rightarrow K^*\gamma$ in 1993 by the CLEO collaboration [6] was the first evidence for $b \rightarrow s$ transitions. The significantly larger dataset now available allows a more precise determination of this branching ratio, the first measurement of charge asymmetries in these decays and the first search for $B \rightarrow \rho\gamma$ and $B^0 \rightarrow \omega\gamma$ decays. In addition we report the first observation of $B \rightarrow K_2^*(1430)\gamma$ decays and the first search for $B^0 \rightarrow \phi\gamma$. This decay can occur through a radiative box diagram

similar to that responsible for $B^0\bar{B}^0$ mixing, but it cannot occur through a radiative penguin transition as the decay $B \rightarrow K^*\gamma$. No branching fraction for this decay has been calculated.

The data were recorded at the Cornell Electron Storage Ring (CESR) with the CLEO detector [7,8]. The results in this Letter are based upon an integrated luminosity of 9.2 fb^{-1} of e^+e^- data corresponding to 9.7×10^6 $B\bar{B}$ meson pairs recorded at the $\Upsilon(4S)$ energy and 4.6 fb^{-1} at 60 MeV below the $\Upsilon(4S)$ energy (“off- $\Upsilon(4S)$ ”). The CLEO detector simulation is based upon GEANT [9]; simulated events are processed in the same manner as the data. The results presented in this Letter supersede the previous CLEO results [6].

Candidates for the decays $B \rightarrow K_{(2)}^*\gamma$ with the subsequent decays $K_{(2)}^{*0} \rightarrow K^+\pi^-$, $K_s^0\pi^0$ and $K_{(2)}^{*+} \rightarrow K^+\pi^0$, $K_s^0\pi^+$ are selected. We reconstruct the decay $B \rightarrow \rho\gamma$ with $\rho^0 \rightarrow \pi^+\pi^-$ and $\rho^+ \rightarrow \pi^+\pi^0$, and $B^0 \rightarrow \omega\gamma$ with $\omega \rightarrow \pi^+\pi^-\pi^0$. We reconstruct $B^0 \rightarrow \phi\gamma$ with $\phi \rightarrow K^+K^-$. Reference to the charge conjugate states is implicit unless explicitly stated otherwise. The charged track and K_s^0 candidates are required to be well reconstructed and to originate near the e^+e^- interaction point. Charged kaons and pions are distinguished using the particle’s measured specific ionization (dE/dx). We require that the dE/dx information, when available, is consistent with the appropriate hypothesis. The K_s^0 candidates are selected through their decay into $\pi^+\pi^-$ mesons. The decay of the K_s^0 candidates is required to be displaced from the e^+e^- interaction point and at least one daughter pion is required to be inconsistent with originating from the interaction point. Neutral pions are reconstructed from photon pairs detected in the electromagnetic calorimeter. The photons are required to have an energy of at least 30 (50) MeV in the barrel (endcap) region, and their invariant mass is required to be within three standard deviations of the π^0 mass [4]. The high energy photon from the radiative B decay is required to have an energy of at least 1.5 GeV and to be in the barrel region $|\cos\theta_\gamma| < 0.71$ where θ_γ is angle between the beam axis and the candidate photon.

The dominant background comes from continuum ($e^+e^- \rightarrow q\bar{q}$ with $q = ucsd$) events with high energy photons originating from initial state radiation (ISR) or $e^+e^- \rightarrow (\pi^0, \eta)X$ with $\pi^0, \eta \rightarrow \gamma\gamma$. The $\cos\theta_\gamma$ requirement reduces the ISR background and the second class of γ background is suppressed by rejecting candidate photons that, when combined with an additional photon candidate, have a mass consistent with the π^0 or η mass [4]. The additional selection criteria described below reduce backgrounds from non-radiative B decays to a negligible level. Background from radiative B decays other than the one under study are discussed later.

We suppress the remaining background from non-radiative B decays and continuum by placing require-

*Permanent address: University of Cincinnati, Cincinnati OH 45221

†Permanent address: Massachusetts Institute of Technology, Cambridge, MA 02139.

‡Permanent address: University of Texas - Pan American, Edinburg TX 78539.

§Permanent address: Yonsei University, Seoul 120-749, Korea.

ments on the observables θ_T (the angle between the thrust axis [10] of the B candidate and the thrust axis of the remainder of the event), θ_B (the angle between the B candidate direction and the beam axis), $M(R)$ and θ_H (the mass and helicity angle of the light meson resonance candidate) and dE/dx . If two or more candidates in an event pass all selection criteria and share daughter tracks or photons, the candidate with smallest deviation from the nominal resonance mass is selected. For the $B \rightarrow \rho\gamma$ analysis, the candidate with smallest $|\cos\theta_B|$ is selected.

Additional background suppression is achieved by requirements on the B candidate energy $\Delta E \equiv E(R) + E(\gamma) - E_{\text{beam}}$ and the beam-constrained B mass $M^2(B) \equiv E_{\text{beam}}^2 - (\mathbf{p}(\gamma) + \mathbf{p}(R))^2$ where the photon momentum $\mathbf{p}(\gamma)$ is rescaled by fixing $E(\gamma) = E_{\text{beam}} - E(R)$. The ΔE resolution of 40 MeV is dominated by the photon energy resolution. The $M(B)$ resolution of 2.8 MeV is dominated by the beam energy spread. We select signal and sideband candidates by requiring $|\Delta E| < 300$ MeV and $5.2 < M(B) < 5.3$ GeV.

We optimize these selection criteria for the $B \rightarrow K_{(2)}^*\gamma$ analyses to maximize $S^2/(S+B)$ where S is the number of expected signal candidates determined from simulated events assuming $\mathcal{B}(B \rightarrow K^*\gamma) = 4.2 \times 10^{-5}$ [4] and $\mathcal{B}(B \rightarrow K_2^*\gamma) = 1.6 \times 10^{-5}$ [11] and B is the number of background candidates determined from off- $\Upsilon(4S)$ data. For the other analyses the selection criteria are optimized to yield the smallest upper limit on the branching fraction on average using the method in [12].

We add the $M(B)$ distributions of the $B^0 \rightarrow (K^+\pi^-)\gamma$ and $B^0 \rightarrow (K_s^0\pi^0)\gamma$ candidates and the $B^+ \rightarrow (K^+\pi^0)\gamma$ and $B^+ \rightarrow (K_s^0\pi^+)\gamma$ candidates requiring $|\Delta E| < 100$ MeV and fit them to obtain the $B^0 \rightarrow K^{*0}\gamma$ and $B^+ \rightarrow K^{*+}\gamma$ yields, respectively (Fig. 1). We perform a simultaneous, binned, maximum-likelihood fit to the two $M(B)$ distributions assuming the signal component is represented by a Gaussian distribution and the background is represented by a threshold function [13]. The fitted yields are $88.3_{-11.5}^{+12.2}$ and $36.7_{-7.6}^{+8.3}$ and correspond to branching fractions of $(4.55_{-0.68}^{+0.72} \pm 0.34) \times 10^{-5}$ and $(3.76_{-0.83}^{+0.89} \pm 0.28) \times 10^{-5}$ for $B^0 \rightarrow K^{*0}\gamma$ and $B^+ \rightarrow K^{*+}\gamma$, respectively. The fractional systematic uncertainties on the measured branching fractions comprise a common uncertainty of 6.8% dominated by the background shape (5%) and the radiative photon detection efficiency (3.3%), and the uncertainties on the reconstruction efficiency of each K^* decay mode that range from 2.6% ($K_s^0\pi^+$) to 5.9% ($K_s^0\pi^0$). We assume $\mathcal{B}(\Upsilon(4S) \rightarrow \bar{B}^0 B^0) = \mathcal{B}(\Upsilon(4S) \rightarrow B^+ B^-) = 0.5$ for all branching fractions in this Letter.

Backgrounds from $B \rightarrow$ charm are negligible and backgrounds from charmless two-body B meson decays are estimated to contribute less than 1.2 and 0.6 events to the $B^0 \rightarrow K^{*0}\gamma$ and $B^+ \rightarrow K^{*+}\gamma$ yields, respectively, based on simulated decays and are neglected in the evaluation of

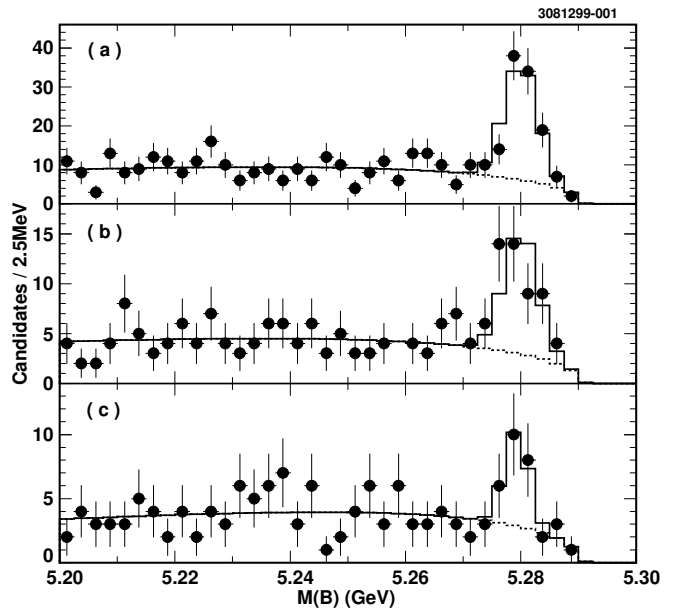


FIG. 1. Beam-constrained B mass distributions for (a) $B^0 \rightarrow K^{*0}(892)\gamma$, (b) $B^+ \rightarrow K^{*+}(892)\gamma$, and (c) $B \rightarrow K_2^*(1430)\gamma$. The data (solid circles) are overlaid with the fit to a Gaussian and background shape [13] (solid line). The fitted background is indicated by the dashed line.

the branching fractions. We have fitted the $M(K\pi)$ distribution summed over K^{*0} and K^{*+} within ± 150 MeV of the K^* mass [4] to search for a non-resonant $B \rightarrow K\pi\gamma$ contribution to the calculated $B \rightarrow K^*\gamma$ yields. No significant non-resonant component with a threshold shape $\propto (M(K\pi) - M(K) - M(\pi))^{1/2}$ is found, but allowing for a non-resonant component would contribute an additional relative uncertainty in the fitted yield of 12%.

We search for direct CP violation by measuring the partial rate asymmetry \mathcal{A}_{CP} ,

$$\mathcal{A}_{CP} \equiv \frac{1}{1-2\eta} \frac{\mathcal{Y}(\bar{B} \rightarrow \bar{K}^*\gamma) - \mathcal{Y}(B \rightarrow K^*\gamma)}{\mathcal{Y}(\bar{B} \rightarrow \bar{K}^*\gamma) + \mathcal{Y}(B \rightarrow K^*\gamma)},$$

where \mathcal{Y} is the fitted yield and η is the mistag fraction. We use the K^* decay modes $K^+\pi^-$, $K^+\pi^0$ and $K_s^0\pi^+$ to measure the CP asymmetry. In these decay modes the charge of the kaon or the K^* contains unambiguous information of the B flavor. Only the $K^+\pi^-$ decay mode has a mistag rate significantly different from zero as determined from simulated events. Mistagging in this mode is due to the 100% transverse polarization of the K^{*0} from $B^0 \rightarrow K^{*0}\gamma$ decays that results in a $\sin^2\theta_H$ distribution. This distribution favors nearly equal momenta of ~ 1.2 GeV/ c for the charged kaon and pion from the K^* . The kaon and pion cannot be kinematically distinguished when $p_K \approx p_\pi$ and their expected dE/dx is nearly identical in this momentum range. We exclude these ambiguous K^{*0} candidates from the \mathcal{A}_{CP} measurement by requiring $|p(K) - p(\pi)| > 0.5$ GeV/ c . This requirement is optimized to give the smallest statis-

tical uncertainty in the asymmetry measurement in the $K^+\pi^-$ decay mode with $\eta = (3.45 \pm 0.02)\%$ determined from simulated events.

The CP asymmetry is determined with a procedure similar to that described for the $B \rightarrow K^*\gamma$ branching fractions. We fit the $M(B)$ distributions of $B \rightarrow K^*\gamma$ and $\bar{B} \rightarrow \bar{K}^*\gamma$ candidates simultaneously for both neutral and charged B meson decays to extract the total yield and asymmetry of both the $B \rightarrow K^*\gamma$ signal and the background in the range $5.2 < M(B) < 5.3$ GeV. For neutral and charged $B \rightarrow K^*\gamma$ decays, we determine $\mathcal{A}_{CP} = -0.13 \pm 0.17$ and $+0.38_{-0.19}^{+0.20}$, respectively, for the signal and -0.03 ± 0.08 and $+0.06 \pm 0.09$ for the background. The asymmetry for the sum of neutral and charged $B \rightarrow K^*\gamma$ decays is $+0.08 \pm 0.13$ [$+0.01 \pm 0.06$] for the signal [background]. Systematic searches for detector- or reconstruction-induced charge asymmetries for charged pions and kaons revealed no significant bias ($|\Delta\mathcal{A}_{CP}| < 1.5\%$). In addition, studies of simulated $B \rightarrow K^*\gamma$ decays indicate that cross-feed between different K^* decays modes is $< 1\%$. Our conservative estimate of the systematic uncertainty on \mathcal{A}_{CP} is 2.5%.

Radiative B meson decays to the K_2^* and the nearby $K^*(1410)$ can be distinguished by the helicity angle distributions ($\propto \cos^2\theta_H - \cos^4\theta_H$ and $\propto \sin^2\theta_H$, respectively) as well as the resonance widths of ~ 100 and ~ 230 MeV [4]. We fit the $M(B)$ distributions of candidates that pass [fail] $|\cos\theta_H|$ requirements designed to enhance [deplete] $B \rightarrow K_2^*\gamma$ decays. The efficiency for passing [failing] the helicity angle requirements is $(10.1 \pm 0.3)\%$ [$(1.09 \pm 0.08)\%$] and $(0.80 \pm 0.13)\%$ [$(0.59 \pm 0.10)\%$] for simulated $B \rightarrow K_2^*\gamma$ and $B \rightarrow K^*(1410)\gamma$ decays, respectively, where the quoted efficiency includes $\mathcal{B}(K_2^* \rightarrow K\pi) = (49.9 \pm 1.2)\%$ and $\mathcal{B}(K^*(1410) \rightarrow K\pi) = (6.6 \pm 1.3)\%$ [4]. The simultaneous determination of $\mathcal{B}(B \rightarrow K_2^*\gamma)$ and $\mathcal{B}(B \rightarrow K^*(1410)\gamma)$ from the two fitted yields and the quoted efficiencies shows that $\mathcal{B}(B \rightarrow K_2^*\gamma)$ is significant at over three standard deviations for the most probable value of $\mathcal{B}(B \rightarrow K^*(1410)\gamma)$ whilst $\mathcal{B}(B \rightarrow K^*(1410)\gamma)$ is less than one standard deviation significant for the most probable value of $\mathcal{B}(B \rightarrow K_2^*\gamma)$. We therefore interpret the signal as being due to $B \rightarrow K_2^*\gamma$ and determine $\mathcal{B}(B \rightarrow K^*(1410)\gamma) < 12.7 \times 10^{-5}$ at 90% CL. The $M(B)$ distribution of $B \rightarrow K_2^*\gamma$ candidates passing the $|\cos\theta_H|$ requirements is shown in Fig. 1(c) summed over the charged and neutral K_2^* meson decays. The fitted yield of $15.9_{-5.1}^{+5.7}$ events is significant at 4.3 [3.3] standard deviations before [after] inclusion of systematic uncertainties. Assuming equal decay rates to charged and neutral K_2^* , the yield corresponds to a branching fraction of $(1.66_{-0.53}^{+0.59} \pm 0.13) \times 10^{-5}$ where the systematic uncertainties are evaluated as described for the $B \rightarrow K^*\gamma$ branching fractions.

The branching fractions of $B \rightarrow K^*\gamma$ and $B \rightarrow K_2^*\gamma$ have been predicted by two groups [11,14]. The

minimal uncertainty is achieved by the ratio $\mathcal{B}(B \rightarrow K_2^*\gamma)/\mathcal{B}(B \rightarrow K^*\gamma) = 0.39_{-0.13}^{+0.15}$ that compares favorably with the prediction of Veseli and Olsson of 0.37 ± 0.10 [11,15] and disagrees with the Ali, Mannel, and Ohl range of 3.0 to 4.9 [14].

In order to limit $|V_{td}/V_{ts}|$, we have searched for the decays $B \rightarrow \rho\gamma$ and $B^0 \rightarrow \omega\gamma$. The $\rho\gamma$ final states suffer from background both from continuum and from $B \rightarrow K^*\gamma$ when a charged kaon is misidentified as a pion. Continuum is the only significant background to $B \rightarrow \omega\gamma$. The ΔE vs. $M(\pi\pi)$ distributions for $B^0 \rightarrow \rho^0\gamma$ and $B^+ \rightarrow \rho^+\gamma$ candidates are shown in Fig. 2 after a requirement of $5274 < M(B) < 5286$ MeV. The K^* background peaks in the lower left hand corner of each distribution whilst the signal peaks near the center and the continuum background is constant. Twenty-four [ten] candidates survive the requirement of $\Delta E > -0.47M(\pi\pi) + 0.32$ GeV [$\Delta E > -0.58M(\pi\pi) + 0.35$ GeV] for $B^0 \rightarrow \rho^0\gamma$ [$B^+ \rightarrow \rho^+\gamma$] as shown in Fig. 2. We estimate the combinatorial background from fits to the $M(B)$ distributions and the background from $B \rightarrow K^*\gamma$ using the measured branching fractions and the reconstruction efficiency from simulated $B \rightarrow K^*\gamma$ decays. The overall reconstruction efficiency is $(12.8 \pm 0.7)\%$ [$(8.5 \pm 0.6)\%$] and the background comprises $9.3_{-0.5}^{+0.6}$ [5.2 ± 0.4] continuum events and 5.4 ± 0.8 [2.6 ± 0.6] $B \rightarrow K^*\gamma$ events for the ρ^0 [ρ^+] decay mode. We determine upper limits of $\mathcal{B}(B^0 \rightarrow \rho^0\gamma) < 1.7 \times 10^{-5}$ and $\mathcal{B}(B^+ \rightarrow \rho^+\gamma) < 1.3 \times 10^{-5}$ at 90% CL. All branching fraction upper limits in this Letter are determined with the method in [12] after reducing the central values of the estimated background, efficiency, daughter branching fractions and number of $B\bar{B}$ pairs by one standard deviation.

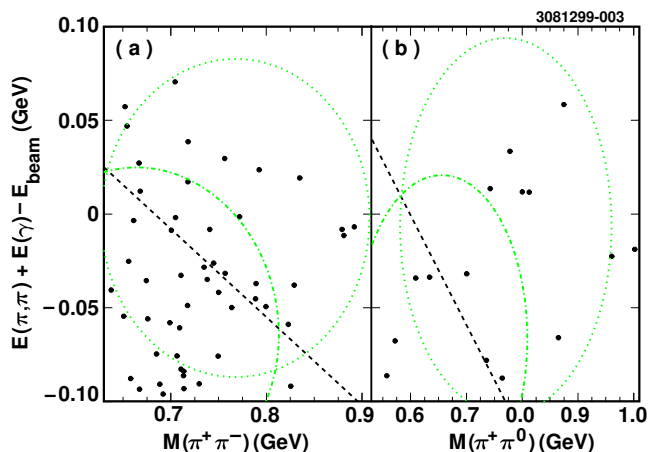


FIG. 2. The ΔE vs $M(\pi\pi)$ distributions for a) $B^0 \rightarrow \rho^0\gamma$ and b) $B^+ \rightarrow \rho^+\gamma$ candidates. Candidates above the diagonal dashed line survive the final selection criterion. The dotted [dot-dash] line approximates the limits that would contain 90% of the $B \rightarrow \rho\gamma$ [$B \rightarrow K^*\gamma$] candidates.

We observe 5 $B^0 \rightarrow \omega\gamma$ candidates in the signal region $|\Delta E| < 100$ MeV and $5274 < M(B) < 5286$ MeV shown

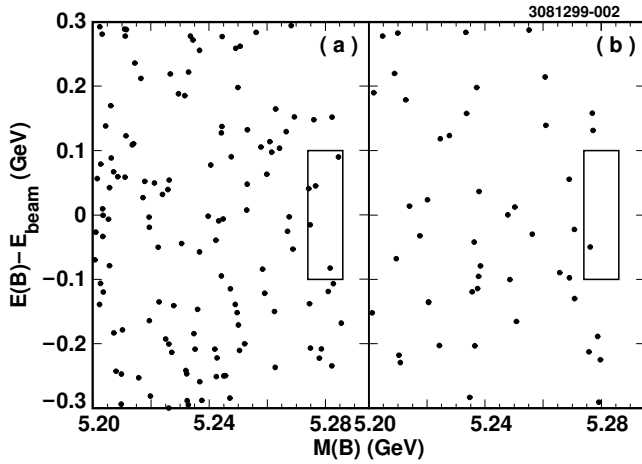


FIG. 3. The ΔE vs beam-constrained B mass distributions for (a) $B^0 \rightarrow \omega\gamma$ and (b) $B^0 \rightarrow \phi\gamma$ candidates. The rectangular area indicates the signal region.

in Fig. 3 (a). The combinatorial background is estimated to be $2.68^{+0.13}_{-0.12}$ from the fit to the $M(B)$ distribution. This corresponds to $\mathcal{B}(B^0 \rightarrow \omega\gamma) < 0.92 \times 10^{-5}$ at 90% CL with the reconstruction efficiency of $(9.7 \pm 0.8)\%$.

The upper limit on $|V_{td}/V_{ts}|$ is derived from the likelihood $\mathcal{L}(R)$ for the ratio $R \equiv \mathcal{B}(B \rightarrow \rho\gamma)/\mathcal{B}(B \rightarrow K^*\gamma) = \xi|V_{td}/V_{ts}|^2$ where $\mathcal{B}(B \rightarrow \rho\gamma) \equiv \mathcal{B}(B^+ \rightarrow \rho^+\gamma) = 2\mathcal{B}(B^0 \rightarrow \rho^0\gamma) = 2\mathcal{B}(B^0 \rightarrow \omega\gamma)$ from isospin symmetry and $\mathcal{B}(B \rightarrow K^*\gamma)$ is the average over B^+ and B^0 decays. The 90% CL limit on R , R_{90} , is given by $\int_0^{R_{90}} \mathcal{L}(R) dR / \int_0^\infty \mathcal{L}(R) dR = 0.90$ where $\mathcal{L}(R) = \prod_i e^{-\mu_i} \mu_i^{n_i} / n_i!$ with $i = \rho^+, \rho^0, \omega$; $n_i =$ total number of $B \rightarrow \rho\gamma$ candidates and $\mu_i = b_i^c + b_i^K + N(B\bar{B})\epsilon_i\mathcal{B}_i^s R\mathcal{B}(B \rightarrow K^*\gamma)$. The estimated continuum [$B \rightarrow K^*\gamma$] background is b_i^c [b_i^K], ϵ_i is the reconstruction efficiency and \mathcal{B}_i^s is the daughter branching fraction. The upper limit of $R < 0.32$ (0.36) implies $|V_{td}/V_{ts}| < 0.75$ (0.79) at 90 (95)% CL for $\xi = 0.58$ [16]. Other estimates of ξ , the ratio of the $B \rightarrow \rho\gamma$ and $B \rightarrow K^*\gamma$ form factors, are 0.77 [17] and 0.81 ± 0.09 [18].

We observe one $B^0 \rightarrow \phi\gamma$ candidate in the signal region $|\Delta E| < 100$ MeV and $5274 < M(B) < 5286$ MeV shown in Fig. 3 (b). We estimate the combinatorial background to be 1.2 ± 0.1 events from the fit to the $M(B)$ distribution. This corresponds to $\mathcal{B}(B^0 \rightarrow \phi\gamma) < 0.33 \times 10^{-5}$ at 90% CL with the reconstruction efficiency of $(23.0 \pm 0.6)\%$.

In summary, the $B \rightarrow K^*(892)\gamma$ branching fractions have been measured with improved precision. A new radiative decay mode $B \rightarrow K_2^*(1430)\gamma$ has been observed and found to agree with one of two theoretical predictions. The partial rate asymmetries in $B \rightarrow K^*(892)\gamma$ decays are measured with a precision of better than 20% and found to be consistent with Standard Model expectations. We find no evidence for the process $b \rightarrow d\gamma$ and determine a limit on the isospin-averaged ratio of

$\mathcal{B}(B \rightarrow \rho\gamma)/\mathcal{B}(B \rightarrow K^*(892)\gamma) < 0.32$ at 90% CL. Using a model-dependent derivation of the ratio of the $B \rightarrow \rho\gamma$ and $B \rightarrow K^*(892)\gamma$ form factors, the ratio of branching fractions implies that $|V_{td}/V_{ts}| < 0.75$ at 90% CL.

We thank A. Ali, T. Mannel, M. Neubert, M.G. Olsson and S. Veseli for useful discussions. We gratefully acknowledge the effort of the CESR staff in providing us with excellent luminosity and running conditions. This work was supported by the National Science Foundation, the U.S. Department of Energy, the Research Corporation, the Natural Sciences and Engineering Research Council of Canada, the A.P. Sloan Foundation, the Swiss National Science Foundation, and the Alexander von Humboldt Stiftung.

-
- [1] We refer to $K^*(892)$ as K^* and $K_2^*(1430)$ as K_2^* .
 - [2] N. Isgur and M.B. Wise, Phys. Rev. D **42**, 2388 (1990).
 - [3] G. Burdman and J.F. Donoghue, Phys. Lett. B **270**, 55 (1991).
 - [4] Particle Data Group, C. Caso *et al.*, Eur. Phys. J. C **3**, 1 (1998) and 1999 off-year partial update for the 2000 edition available on the PDG WWW pages (URL: <http://pdg.lbl.gov/>).
 - [5] L. Wolfenstein and Y.L. Wu, Phys. Rev. Lett. **73**, 2809 (1994); H.M. Asatrian and A.N. Ioannissian, Phys. Rev. D **54**, 5642 (1996); A.L. Kagan and M. Neubert, Phys. Rev. D **58**, 094012.
 - [6] CLEO Collaboration, R. Ammar *et al.*, Phys. Rev. Lett. **71**, 674 (1993).
 - [7] CLEO Collaboration, Y. Kubota *et al.*, Nucl. Instrum. Methods A **320**, 66 (1992).
 - [8] T. Hill, Nucl. Instrum. Methods A **418**, 32 (1998).
 - [9] R. Brun *et al.*, GEANT 3.15, CERN Report No. DD/EE/84-1 (1987).
 - [10] E. Farhi, Phys. Rev. Lett. **39**, 1587 (1977).
 - [11] S. Veseli and M.G. Olsson, Phys. Lett. B **367**, 309 (1996).
 - [12] G. Feldman and R. Cousins, Phys. Rev. D **57**, 3873 (1998).
 - [13] $f(x) \propto x\sqrt{1-x^2} \exp(\kappa(1-x^2))$ where $x \equiv M(B)/E_{\text{beam}}$. The parameter κ is determined by the fit. ARGUS Collaboration, H. Albrecht *et al.*, Phys. Lett. B **241**, 278 (1990); **254**, 288 (1991).
 - [14] A. Ali, T. Ohl, and T. Mannel, Phys. Lett. B **298**, 195 (1993).
 - [15] The uncertainty on the ratio of branching fractions is dominated by the additional fractional uncertainty in $\mathcal{B}(B \rightarrow K_2^*\gamma)$, M. G. Olsson, private communication.
 - [16] A. Ali, V.M. Braun, and H. Simma, Z. Phys. C **63**, 437 (1994).
 - [17] S. Narison, Phys. Lett B **327**, 354 (1994).
 - [18] J. M. Soares, Phys. Rev. D **49**, 283 (1994).